euspen's 22nd International Conference & Exhibition, Geneva, CH, May/June 2022
www.euspen.eu

# Investigations on the tracking control and performance of a long stroke vertical nanopositioning drive

Alex S. Huaman[1], Stephan Gorges[1], Michael Katzschmann[1], Steffen Hesse[1], Thomas Fröhlich[2], Eberhard Manske[2]

[1] *IMMS Institut für Mikroelektronik- und Mechatronik-Systeme gemeinnützige GmbH (IMMS GmbH), 98693 Ilmenau, Germany*
[2] *Institute of Process Measurement and Sensor Technology, Technische Universität Ilmenau, 98693 Ilmenau, Germany*

*{alex.huaman, stephan.gorges, michael.katzschmann, steffen.hesse}@imms.de, {thomas.froehlich, eberhard.manske}@tu-ilmenau.de*

**Abstract**
This paper presents an approach to equip an existing planar nanoprecision drive system with specially designed lifting and actuating units (LAUs), which can lift several kilograms along a vertical stroke of 10 mm with nanometer precision. These modules contain a pneumatic actuator to counteract the weight force along the entire travel range without introducing significant heat into the measurement space. An additional parallel acting electromagnetic actuator provides the precision positioning forces.
As an initial step toward a full 6D system, each LAU is set up individually on a test bench. Using an included laser interferometric measurement system and emulated loads, allows for the development and evaluation of different control strategies within the simulation framework and via real-time experiments.
Designing a controller for a single LAU involves an in-depth research into its overactuated nature and the derivation of a detailed model of the drive as well as the motion system. The proposed control strategy achieves subnanometer precision by integrating a feedforward stage for trajectory tracking and an output-feedback stage for stabilization and disturbance rejection. In this context, the output-feedback controller highlights a composite state and disturbance observer. In order to accomplish an adequate tradeoff between performance and robustness, the controller tuning is performed in the time and frequency domain based on systematic LQR/LQG design methods. The effectiveness of the presented control strategy is verified via real-time experimentation, where the overall control scheme allows RMS positioning errors below 0.3 nm which seem to be dominated by the measurement noise. Moreover, it renders very low heat dissipation of about 54 nW to carry a 4 kg payload.

Keywords: nanopositioning and nanomeasuring machines, nanofabrication, vertical drives, weight force compensation, overactuated systems, feedforward and feedback control

## 1. Introduction

The ever-advancing miniaturization of micro- and nanosystems poses new challenges for the positioning systems involved. In this context, the authors are investigating the design and control of nanopositioning systems with large travel ranges on the basis of a multicoordinate direct drive approach. Such as the NPPS100, a nanopositioning system, utilizing planar aerostatic guiding, laser interferometers (LIFs), and a 3D direct electromagnetic drive to position a sample in a ⌀100 mm planar range with nanometer precision [1].

Due to the limited flatness of the massive granite base, tilting errors around the planar $x$- and $y$-axis and vertical $z$-position errors are introduced. To counteract these errors, this drive system needs to be upgraded by implementing vertical actuation, thereby transitioning to a 6D system as shown in Figure 1. Despite the existing vertical-acting axis for precision tasks [2], further information like the maximum load capacity, travel range, and how lifting modules will influence a planar drive system was reported in [3] using purpose-designed lifting and actuating units (LAUs). Hereinafter, three LAUs are mounted, one on each corner. The vertical range is projected to cover 10 mm in order to increase the functionality of the drive system. Moreover, in [3] it was shown that this concept is feasible and worth further investigation in metrology, nanofabrication, and nanopositioning applications.

## 2. Design of the Lifting and Actuating Units

The design of the LAUs used in this paper has been described in depth in [4], therefore here only an overview is given.

The major task of the LAUs is to move the sliders and specimens mass (total of 12 kg) in a vertical range of 10 mm. Due to the overall symmetric design, the loads are distributed evenly, thus three identical LAUs can be used.

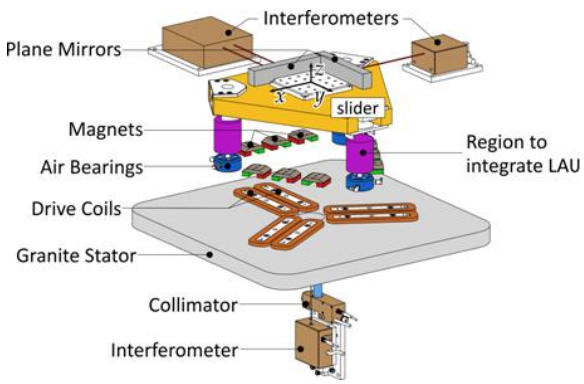


**Figure 1.** Explosional view of the NPPS100-6D. [5]

The aim is to achieve precision and dynamics comparable to the planar performance (i.e., 250 mm/s², 1 nm RMS-position error [1]). Each LAU needs to fit into a space of just ⌀50 mm

across by 60 mm in height. Therefore, all components need to be tightly integrated. As with most precision systems, the heat introduced into the measurement space should be kept to a minimum, due to thermal expansion and large time constants.

The investigation did not yield a single actuation method that fulfills both low heat output and a large travel range for the given load. Therefore, an additional thermally passive weight force compensation (WFC) is introduced. This device only counteracts the static weight force thus, the primary actuator only needs to create the precision motion forces. The WFC dynamics are mostly irrelevant, but it needs to be adjustable to different payloads. It was found that a pneumatic piston as a WFC and a Lorentz force drive as a precision actuator complement each other very well. The WFC is implemented as a pneumatic piston which is sized according to the weight force and the desired equilibrium pressure. For the precision Lorentz force actuator, numerous FE-models and optimization cycles were evaluated to find the optimal geometry. The force-to-power ratio $F2P$ was used as the objective function since it is the major performance parameter for an efficient linear electromagnetic drive. In the end, a drive geometry with a $F2P$ of more than 60 N²/W was found.

An aerostatic vertical guiding is integrated into the piston to achieve a frictionless and stick-slip-free motion. Further, a sensitive optical linear encoder is used in each LAU to be able to initialize the global LIFs. Additionally, the encoder can be utilized as a fallback system in case of a laser beam break. All these functional components of a single LAU are illustrated in Figure 2.

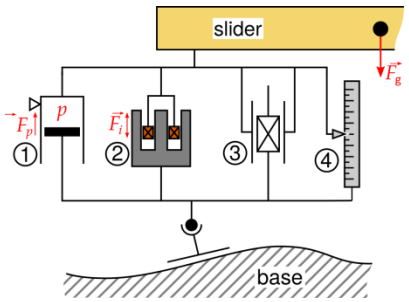


**Figure 2**. Functional components of each LAU: (1) pneumatic WFC (2) precision Lorentz force actuator, (3) vertical guiding, (4) internal measurement system. [3]

### 3. Single Degree of Freedom Test Setup

For evaluating and optimizing the projected performance of a single LAU a test bench with a single degree of freedom was set up. An overview of the mechanical system is given in Figure 3. It is situated on a passive vibration-isolating granite stator. A single LAU is mounted at one corner of the slider dummy, while the other corners are hinged on a secondary support system. The vertical displacement is measured through a high-precision laser interferometer with a resolution of 20 pm, provided by SIOS GmbH. To this end, a fixed mirror is placed in the center of the slider. For precise measurements, the reflected beam must be coincident with the outgoing beam, i.e., the slider with the mirror must be adjusted precisely perpendicular to the LIF with an angular tolerance of about ±30". This latter statement is helpful for the linearization of the model dynamics and, in addition, restricts the maximum vertical displacement up to 80 µm maximum. To change the working height to a larger range up to 10 mm, the secondary support system needs to be adjusted manually.

Figure 4 depicts the functional test-bench diagram. For data acquisition and rapid control prototyping, a dSpace real-time board is used in combination with Matlab/Simulink and ControlDesk. The analog outputs of the real-time board supply the setpoint values for the coil current and pneumatic WFC. This is physically realized through voltage (±10 V) with 16-bit resolution. These setpoints are converted into real magnitudes using a power amplifier unit and a pneumatic supply unit, respectively. The displacement is measured by the LIF and collected via the digital peripherals of the dSpace board.

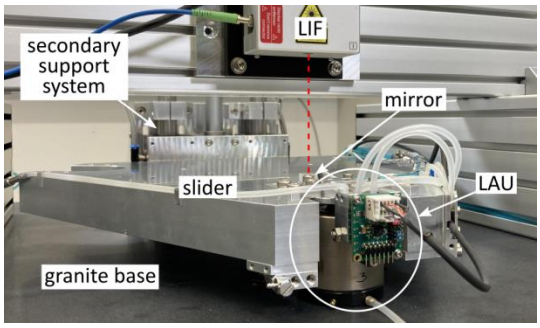


**Figure 3.** Overview of the 1D mechanical test setup.

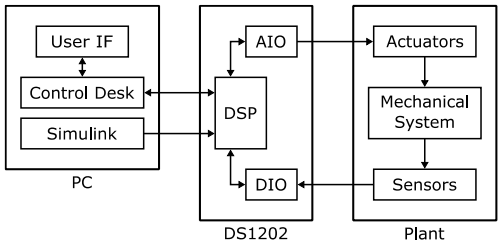


**Figure 4.** Overview of the real-time environment.

### 4. Model and Controller Derivation

Investigations on positioning and tracking control focus on the design of output-feedback controllers considering the only available measurement signal, i.e. the position signal. The starting point for the controller design is the derivation of a detailed model. At this point, it results instrumental to derive and identify models which characterize the dynamic behavior of the motion system (or plant), comprising the mechanism, actuators, sensors, and perturbations. The main component of the plant is the LAU with its pneumatic WFC and Lorentz force actuator. Due to the conservatism of the pneumatic actuator, its performance is limited to a quasi-static operation and, for simplicity, its dynamics can be neglected. The force equation for the pneumatic actuator reads

$$F_p(t) = A_\mathrm{r} p(t), \tag{1}$$

where $p$ is the relative air pressure, $A_\mathrm{r}$ is the cross-sectional area of the piston, and $F_p$ is the resulting force. On the other hand, the parameter that reflects the amount of current required to create a given force is the motor constant, i.e.

$$F_i(t) = K_\mathrm{m}(z) i(t). \tag{2}$$

This force-to-current ratio exhibits a parabolic behavior varying as a function of the vertical displacement of the LAU, see Figure 5. Finally, the overall input force of the plant reads

$$F(t) = F_p(t) + F_i(t) - F_\mathrm{g} = K_\mathrm{m} i(t) + A_\mathrm{r} p(t) - F_\mathrm{g}, \tag{3}$$

where $F_\mathrm{g}$ is a matched gravitational force perturbation.

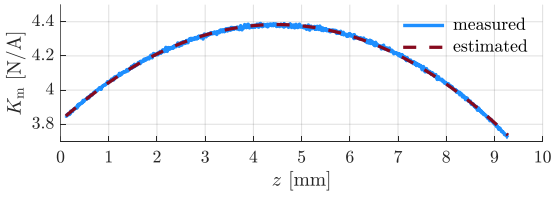


**Figure 5.** Motor constant variation w.r.t. the vertical displacement.

It is interesting to notice that the plant features more complex dynamics owing to its overactuated nature and due to the fact that it includes additional unmodeled mechanical components. However, it is possible to characterize the plant using a single force as input, being reduced into a SISO system. Towards this end, the Frequency-Apportioned Control Allocation (FACA) method [6] takes place to guarantee the control performance of the slowly-varying WFC, as well as the highly dynamic Lorentz force actuator, while dealing with a single control signal. The key element in this approach is the appropriate selection of the low-pass filter, as shown in [7]. It is noteworthy to mention that the constant $A_\mathrm{r}$ and polynomial $K_\mathrm{m}$ ratios will be useful later to transform the forces $F_p$ and $F_i$ into pneumatic pressure $p$ and current $i$, respectively.

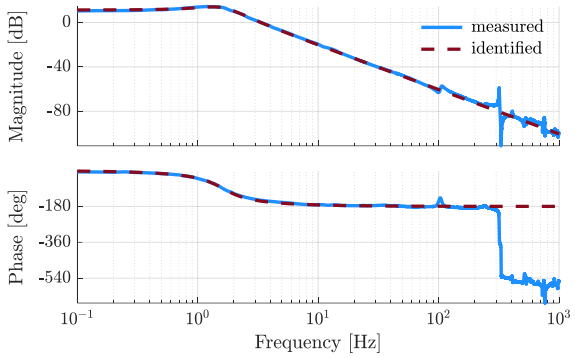


**Figure 6.** Frequency response function of the plant at 1 mm levitation height (input: force [N], output: vertical displacement [mm]).

Given that the dynamics of the plant are dominantly linear, the frequency response function (FRF) is measured in order to get a closer look at the resonance modes of the plant [8]. Figure 6 illustrates in light blue the measured FRF and in dark red the identified model. Here, up to a frequency of approximately 90 Hz, the identified model closely matches the first resonance mode. In addition, an anti-resonance followed by a resonance peak can be observed in the range from 90 Hz to 110 Hz, and *vice-versa* around 310 Hz. The aforementioned vibration modes describe the internal dynamics associated with the plant and are produced due to structural modes. However, the study of these (internal) dynamics and structural modes is beyond the scope of the present paper. Through the application of system identification tools [9], a stable, linear, time-invariant, and slightly underdamped second-order model is obtained, which captures most of the relevant dynamics of the plant and, therefore, is instrumental for controller design.

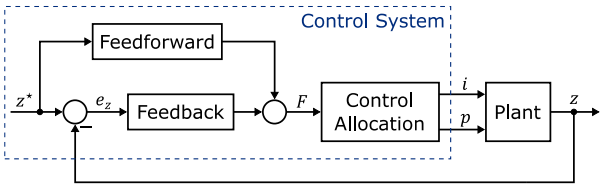


**Figure 7.** Overall control architecture.

The control system design is subsequently studied and implemented. This nominal (or baseline) controller is meant to achieve sub-nanometer accuracy by integrating a feedforward controller for trajectory tracking and an output-feedback controller for stabilization and active disturbance rejection. The output-feedback controller highlights a composite state and disturbance observer. The core of the feedback law consists of an LQG-type controller based on [10]. In order to accomplish an adequate tradeoff between performance and robustness, the controller tuning is performed in the time and frequency domain based on systematic LQR/LQG design methods. In Figure 7 the functional closed-loop system is depicted. A further element to consider in the controller design is the control allocation stage [6]. This block is responsible for splitting a single control signal $F$ into current $i$ and pneumatic pressure $p$, see Figure 7. For further details and discussion about the controller derivation for this class of high-precision motion systems, the reader is referred to [10] and [11].

## 5. Performance Evaluation

For real-time experiments, the control algorithms are running using a sampling rate of 10 kHz. For the sake of brevity, most of the real-time experiments reported here were performed at 1 mm levitation height. It is noteworthy that measurements with the slider set down and resting on the massive granite stator highlighted a remaining position noise of about 0.22 nm (RMS), which represents a limitation for the achievable controller performance. In closed-loop operation (i.e, including aerostatic guiding, pneumatic WFC, electromagnetic precision drive, and active controller) the standard deviation (or RMS) error remains below 0.30 nm. Figure 8 depicts the time series of a steady-state positioning exercise over a time span of 10 s. Here the RMS positioning error is as low as 0.29 nm and seems to be dominated by the position and signal noise, while a suitably low current is achieved. Subsequently, direct and straightforward calculations reveal that the implemented control system renders a very low heat dissipation of about 54 nW for carrying a payload of 4 kg approximately.

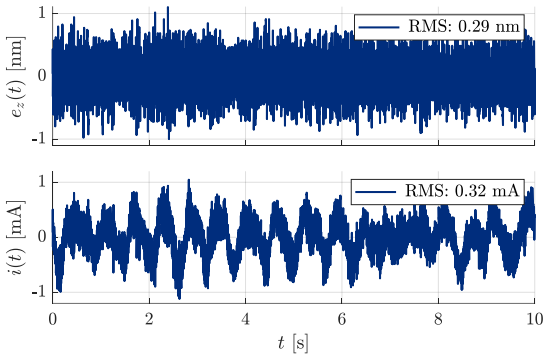


**Figure 8.** Time series of the closed-loop positioning error and control current at 1 mm levitation height.

For the sake of completeness, further measurements were also performed over the macroscopic travel range of the module. Figure 9 presents the height-dependent changes in RMS, proving that the overactuated vertical motion system provides subnanometer accuracy along its vertical stroke of about 10 mm. Here, the RMS positioning error and the RMS control current remain below 0.30 nm and 0.35 mA, respectively. Given the very low current, the biggest shortcoming for lifting modules with nanometer precision, i.e. heat emission, is minimized by emitting only a few nanowatts of heat into the measurement space. The traced data underlines that the closed-loop system achieves outstanding performance in steady-state positioning applications.

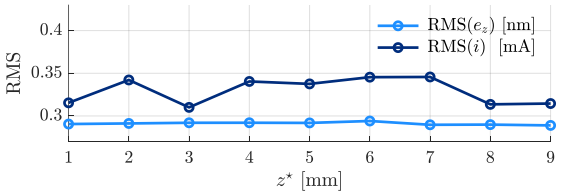


**Figure 9.** RMS deviation w.r.t. the vertical displacement.

For trajectory tracking exercises, two assumptions were met prior to choosing the trajectory, i.e., (i) the initial states were carefully chosen in order to avoid the computation of huge control signals at the beginning of the experiment, and (ii) the rate of motion and mechanical constraints were also considered. Subsequently, motion profiles were designed as illustrated in Figure 10, i.e., a point-to-point trajectory with a so-called *double-S* velocity profile [12]. Despite the *double-S* trajectory is widely used in industrial applications and provides continuous acceleration profiles, these profiles are trapezoidal and, therefore, have non-differentiable points leading to undesired excitation of resonance frequencies.

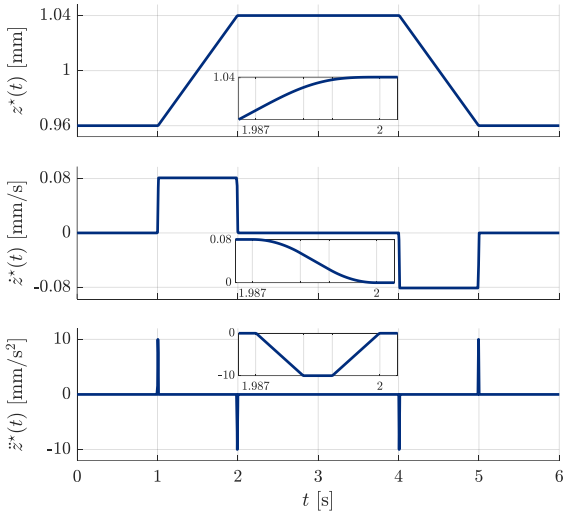


**Figure 10.** Point-to-point *double-S* trajectories for the generation of vertical displacement.

The effectiveness of the control allocation method [6] for heat emission minimization is examined next. To this end, two cases were addressed. The first case, subsequently called passive WFC, corresponds to hold (or freeze) the pneumatic pressure, such that all control effort will be allocated to the current while the pneumatic pressure remains constant. The second case, or active WFC, corresponds to letting the control allocation in operation without modifying it. Figure 11 depicts the traced data for the two cases discussed above. Here, the passive WFC is plotted in dark blue and the active WFC in light blue. For all cases, high-precision control and disturbance rejection are handled by the electromagnetic drive.

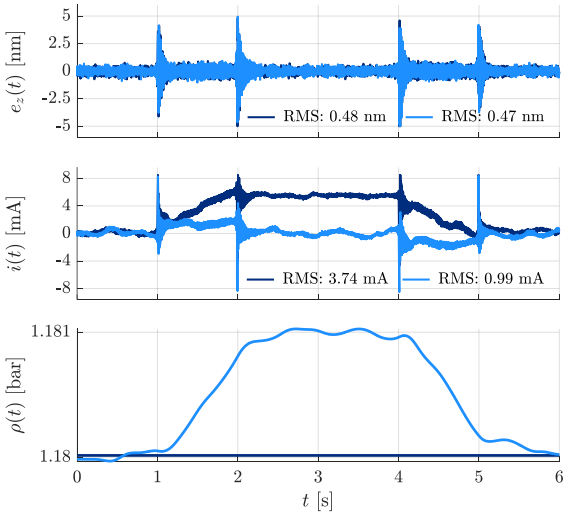


**Figure 11.** Trajectory tracking exercises. Pneumatic WFC: (i) passive case in dark blue and (ii) active case in light blue.

It is noteworthy that in both cases, the RMS tracking error is practically unchanged; however, there exists a significant difference in the RMS control current. A passive WFC produces an increment in the current when the system is driven to a different height, this higher current is reflected in an undesirable increment of heat emission. Despite this unwanted heating fact, the tracking errors remain comparable.

## 6. Conclusion

The initial operation performance validates the design concept, where the overactuation given by the pneumatic piston and the (almost zero) current in the coil work as expected. The effectiveness of the implemented model-based nominal controller has been verified via real-time experiments, where the overall control scheme yields RMS positioning errors below 0.30 nm, which seems to be dominated by the position and signal noise. Emphasis is placed on the tracking exercises and the control allocation method. The latter proves to be adequate for the application since it demands a low computational cost and avoids heat emission via low current. Future research will explore the adaptive augmentation of the nominal controller, and is expected to enhance the tracking performance even further via internal dynamics analysis.


## Acknowledgments

The authors gratefully acknowledge the financial support from the Deutsche Forschungsgemeinschaft (DFG) in the framework of the Research Training Group “Tip- and Laser-Based 3D-Nanofabrication in Extended Macroscopic Working Areas” (GRK 2182) at the Technische Universitat Ilmenau, Germany.


## References


[1] Hesse S, Schäffel C, Mohr HU, Katzschmann M, and Büchner HJ 2012 Design and performance evaluation of an interferometric controlled planar nanopositioning system *Measurement Science and Technology* **23** 074011

[2] Eitzenberger H and Harnisch J 2014 Positioning device, x-y table, and lifting unit *WO2014090291A1*

[3] Gorges S, Hesse S, Schäffel C, Ortlepp I, Manske E, Langlotz E, and Dontsov D 2019 Integrated planar 6-DOF nanopositioning system *IFAC Mechatronics/ NOLCOS* 838-843

[4] Gorges S 2020 A Lifting and actuating unit for a planar nanoprecision drive system (PhD thesis) *Technische Universität Ilmenau*

[5] Gorges S 2021 Hubmodule für die Präzisionsantriebstechnik *Konstruktion* **11-12** 36-40

[6] Davidson J B, Lallman F J, and Bundick WT 2001 Integrated reconfigurable control allocation *AIAA Guidance, Navigation and Control Conference and Exhibit* 1-11

[7] Sadien E, Roos C, Birouche A, Carton M, Grimault C, Romana L E, and Basset M 2020 A simple and efficient control allocation scheme for on-ground aircraft runway centerline tracking *Control Engineering Practice* **95** 104228

[8] Pintelon R and Schoukens J 2012 System identification: a frequency domain approach *John Wiley & Sons*

[9] Forssell U and Ljung L 1999 Closed-loop identification revisited *Automatica* **35(7)** 1215-1241

[10] Huaman A S, Katzschmann M, Hesse S, Schaeffel C, Weise C, Dontsov D, Manske E, and Reger J 2021 Picometer-scale positioning of a linear drive system via feedforward-feedback control *IEEE International Conference on Mechatronics (ICM)* 1-6

[11] Treichel K 2017 Modeling and robust adaptive tracking control of a planar precision positioning system (PhD thesis) *Technische Universität Ilmenau*

[12] Biagiotti L and Melchiorri C 2008 Trajectory planning for automatic machines and robots *Springer Science & Business*